# Voltage-dependent electron distribution in a small spin valve: Emission of nonequilibrium magnons and magnetization evolution

V. I. Kozub
*A.F. Ioffe Physico-Technical Institute, St.-Petersburg 194021, Russia Federation*

J. Caro
*Kavli Institute of NanoScience Delft, Delft University of Technology, Lorentzweg 1, 2628 CJ Delft, The Netherlands*
(Received 16 July 2007; published 21 December 2007)

We describe spin transfer in a ferromagnet/normal metal/ferromagnet spin-valve point contact. Spin is transferred from the spin-polarized current to the magnetization of the free layer by the mechanism of incoherent magnon emission. Our approach is based on the rate equation for the magnon occupation, using Fermi's golden rule for magnon emission and absorption and the nonequilibrium electron distribution for a voltage-biased spin valve. The magnon emission reduces the magnetization of the free layer. Depending on the sign of the applied voltage for parallel or antiparallel magnetizations, a magnon avalanche, characterized by a diverging effective magnon temperature, sets in at a critical voltage. This critical behavior can result in magnetization reversal and consequently to suppression of magnon emission. However, magnon-magnon scattering can lead to saturation of the magnon concentration at a high but finite value. The further behavior depends on the parameters of the system. In particular, gradual evolution of the magnon concentration followed by magnetization reversal is possible. Another scenario is the steplike increase of the magnon concentration followed by a slow decrease. In this scenario a spike in the differential resistance is expected due electron-magnon scattering. Then, a random telegraph noise in the magnetoresistance can exist, even at zero temperature. A comparison of the obtained results to existing theoretical approaches and experimental data is given. We demonstrate that our approach for magnetization configurations close to collinear corresponds to the voltage-controlled regime. Namely, the magnetization evolution is related to nonequilibrium spin-dependent electron distribution controlled by the total voltage applied to the device. In this regime the evolution has an exponential character. In contrast, the existing spin-torque approach corresponds to a current-controlled regime, and the evolution rate is restricted by value of the total spin current through the "analyzing" ferromagnetic layer. It is shown that our scenario dominates at mutual magnetization orientation close to the parallel or antiparallel.

DOI: 10.1103/PhysRevB.76.224425 PACS number(s): 75.40.Gb, 75.47.De, 75.30.Ds, 85.75.Bb

## I. INTRODUCTION

Presently, there is a strong interest in the magnetization dynamics of small spin-valve devices induced by a spin-polarized current traversing the magnetic layers. This dynamics has important application potential. For example, it may be used for current-controlled switching of magnetic random access memory elements and for microwave oscillators, the latter devices being based on steady-state magnetization precession.

In this field the key topics are the mechanism by which spin is transferred from the polarized current to the magnetization of the relevant layer and the description of the resulting magnetization dynamics in dependence of bias current, bias voltage, and magnetic field. The initial predictions for these phenomena were made by Slonczewski[1] and Berger.[2] The theory of the former, also termed spin-torque theory, attracts more interest. According to Ref. 1 spin transfer should lead to steady, coherent precession of the magnetization of the layers and, in the presence of a uniaxial anisotropy, to switching of the magnetization and thus to an abrupt change of the resistance of the structure. These effects should occur for high current densities ($10^6$–$10^7$ A/cm$^2$) and small lateral dimensions ($\approx$100–1000 nm).

The initial experiments on this magnetization switching are reported in Refs. 3–5. The results in Refs. 3 and 5 are interpreted in the framework of Slonczewski's theory. In addition to switching, these studies also show gradual behavior in the traces of the (differential) resistance versus current, which cannot be explained by theory.[1] The traces in Ref. 5 are hysteretic at low applied magnetic field (in accordance to theory[1]), but at higher field they show nonhysteretic spikes, which are attributed to precession states. Such states can also manifest themselves by the emission of microwave radiation, as demonstrated in Refs. 6–8. Similar experimental results on switching and spikes are described in Ref. 9, which in addition reports random telegraph noise in time traces of the resistance. The latter is interpreted as resulting from transitions between two metastable magnetic states separated by a barrier. It is suggested that the transition kinetics is determined by the temperature defined by magnetic excitations (magnons) induced by the spin current. Considerations supporting this idea were given in Refs. 10 and 11. Random telegraph noise is also reported in Refs. 12 and 13, where it is ascribed to regular thermal activation (i.e., involving the equilibrium temperature of the system) over the barrier. Corresponding theoretical models are presented in Refs. 14 and 15. Note that thermal activation involving the equilibrium temperature cannot apply to the noise in Ref. 9, since this was also observed at 4.2 K (Refs. 12 and 13 apply to room temperature), where thermal activation is virtually absent. In connection to this short history of the field, it is noted that

 

the very idea that the evolution of the magnetic state of a spin valve or multilayer system of nanoscale lateral dimension may arise from generation of nonequilibrium magnons was first formulated in Ref. 4, mostly in a qualitative picture.

So far, analysis of magnetic switching in small spin valves is almost exclusively based on the spin-torque theory.[1] Although the description of spin transfer from the electrons to the magnetization was subsequently refined in Refs. 17–24, the principal concepts describing the evolution of the magnetic state of the layer are still those of Ref. 1. In Refs. 22–24 the idea that damping of magnetization precession should be of electronic nature is an important ingredient. In Ref. 22 an expression for the Gilbert damping parameter is calculated. The mechanism relies on transfer of spin from the precessing magnetization of the magnetic layer to the electrons incident on the normal metal layer and subsequent diffusion of this spin into the normal layer. Actually, the process of spin decay is considered as related to interface effects, implying that the damping parameter decreases as the layer thickness increases.

Although it accounts for many important experimental features, approach[1] fails to explain the aforementioned gradual evolution of the magnetization, activated behavior at low temperatures, and precession states with small precession angles.[7] Such precession states present a problem for theory,[1] since the Landau-Lifshitz equation, which is at the basis of Ref. 1 implies large precession angles.[5,25,26]

The approach in Ref. 1 is semiclassical: The electron spin is treated quantum mechanically, but spin transfer is derived from the classical law of angular momentum conservation. This approach is inapplicable if initially the system is in a pure parallel or pure antiparallel configuration, since then the spin-torque vanishes. In these cases the initial stage of evolution is naturally controlled by quantum fluctuations, i.e., by magnons. Further, in Ref. 1 it is ignored that in the spin-transfer regime the electron system is strongly out of equilibrium. Actually, the spin-transfer regime is reminiscent of point-contact spectroscopy (PCS) of the electron-magnon interaction in ferromagnetic metals, which was theoretically developed by Kulik and Shekhter[27] for homogeneous ferromagnetic point contacts. The idea is that in a biased point contact a nonequilibrium electron distribution is created. This distribution enables energy relaxation of the electrons by incoherent emission of magnons, the elementary excitations of magnetization. Magnon emission can be probed[28] in the electrical characteristic of the contact. In the same spirit, a nonequilibrium electron distribution created in a biased spin valve should lead to incoherent emission of magnons in the magnetic layer(s). This results in a change of the magnetization, which can be detected in the giant magnetoresistance. To some extent Berger[2] discusses a nonequilibrium distribution, but his intuitive approach lacks a solid quantum mechanical basis.

In this article we present a consistent quantum mechanical description of spin transfer in a spin-valve point contact, based on Fermi's golden rule and taking into account the nonequilibrium electron distribution. Similar to PCS of the electron-magnon interaction,[27,28] we consider emission and absorption of magnons. However, contrary to PCS, which is concerned with the effect of electron-magnon processes on electrical transport, we here focus on the effect of these processes on the magnetization, which can be strongly reduced by a nonequilibrium population of emitted magnons. We show that different scenarios of the magnetization evolution are possible, including switching, gradual evolution of the magnetization, hysteretic and reversible behavior, precession states with small precession angles, as well as two-level fluctuations at zero temperature. Further, electronic Gilbert damping, derived in Ref. 22 in a cumbersome way, in our model appears straightforwardly. Moreover, we show that in crystalline ferromagnetic layers with elastic scattering the damping is of bulk rather than surface nature. The scenario of magnon emission and absorption presented below does not contradict the recent observation of nanomagnet dynamics in the time domain,[16] which shows nearly coherent magnetization precession.

Comparing our approach to the spin-torque approach, we will demonstrate an important difference between them. Namely, in our approach the electron distribution is strongly out of equilibrium and is completely controlled by the applied voltage, irrespective of the current through the structure. We call the corresponding regime the *voltage*-controlled regime. We show that it holds for small precession angles, i.e., close to antiparallel or parallel mutual orientation of the magnetization of the layers. In contrast, the spin-torque model ignores the nonequilibrium distribution, while the magnetization evolution is ascribed to spin pumping by the incident spin current. It turns out that the corresponding regime is a *current*-controlled regime. We discuss in detail the relation between the two regimes and the possible crossover between them in the course of the magnetization evolution. In particular, our scenario (definitely describing small precession angles) can cross over to the semiclassical evolution according to theory,[1] which can only describe large precession angles.

## II. EMISSION OF MAGNONS

### A. Device geometry and electron-distribution function

The point contact we consider has two planar electrodes making electrical contact via a nanohole of diameter $d$ in a thin insulator (see Fig. 1). In the left electrode there is a spin valve of structure $F(t_p)\ N(t_{sp})/F(t_a)$, the layers acting as spin-polarizer ($p$), spacer ($sp$) and spin-analyzer ($a$), respectively ($F$=ferromagnet; $N$=normal metal). Typically, the thicknesses are such that $t_p > t_a \approx t_{sp}$, while $t_p$ is smaller than the inelastic diffusion length and spin diffusion length. The polarizer's magnetization $\mathbf{M}_p$ points in the positive $z$ direction, while the analyzer's magnetization $\mathbf{M}_a$ is antiparallel or parallel to $\mathbf{M}_p$. Both polarizer and analyzer are single domain layers. The $N$ spacer is much thinner than the spin-flip diffusion length (and any other scatter length) in the $N$ spacer, so that spin is preserved between polarizer and analyzer. The $N$ layer between analyzer and insulator is thin (thickness $\approx t_{sp}$). Apart from the insulator all further material is $N$ as well. The different scattering of the minority- and majority-spin channels in the $F$ layers is reflected in the resistivities $\rho_F^{\min}$ and $\rho_F^{\mathrm{maj}}$, which obey $\rho_N \ll \rho_F^{\mathrm{maj}} < \rho_F^{\min}$ ($\rho_N$ is the $N$ resistivity). The elastic mean free path of the electrons, both in $N$

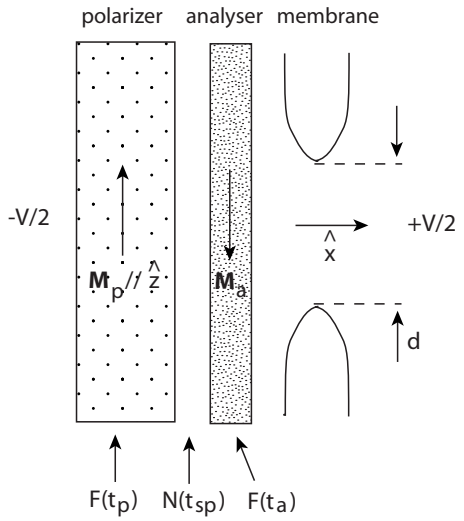


FIG. 1. Point contact with a spin valve located in the left electrode, adjacent to the insulator with a nanohole. The magnetization $\mathbf{M}_p$ of the polarizer is fixed and points in the positive $z$ direction, while the magnetization $\mathbf{M}_a$ of the analyzer points either in the positive or the negative $z$ direction. From the polarizer a spin-polarized current is incident on the analyzer. The axis of the point contact is the $x$ axis. Further details are discussed in the text.

and $F$, is smaller than the size of the nanohole, so that transport is diffusive.

The device is positively biased at voltage $V$ $(V>0)$, applying $-V/2$ to the left electrode and $+V/2$ to the right electrode. This gives a spin-polarized electron current from polarizer to analyzer. In zeroth order, i.e., without inelastic processes, the resulting spin-dependent electron-distribution function in the plane of the orifice (and to a good approximation in the analyzer, since it is so close to the orifice) is

$$f_{\mathbf{k},\sigma} = \frac{1}{2}\left\{\left[1-\alpha\left(\frac{1}{2}+\sigma\right)\right]f_0\left(\epsilon_{\mathbf{k},\sigma}+\frac{eV}{2}\right) + \left[1+\alpha\left(\frac{1}{2}+\sigma\right)\right]f_0\left(\epsilon_{\mathbf{k},\sigma}-\frac{eV}{2}\right)\right\}. \quad (1)$$

Here $\alpha=\Delta R_p/R_M=4(\rho_{\mathrm{FM}}^{\mathrm{min}}-\rho_{\mathrm{FM}}^{\mathrm{maj}})t_p/(\pi d^2 R_M)$ is the spin-polarization induced by the polarizer. This estimate is based on the assumption that the total device resistance is dominated by $R_M$, while the polarizer resistance is relatively small. It is written in terms of polarizer resistances seen by minority-spin and majority-spin electrons, normalized to $R_M=\rho_N/d$, which is the Maxwell resistance of the corresponding diffusive, homogeneous $N$ point contact. The parameter $\sigma$ denotes the electron spin in the polarizer, where majority spins have $\sigma=+1/2$ and minority spins have $\sigma=-1/2$. When $\mathbf{M}_p$ and $\mathbf{M}_a$ are antiparallel, $\sigma=+1/2$ in Eq. (1) gives the minority distribution in the analyzer, while $\sigma=-1/2$ gives the majority distribution in that layer. For the parallel configuration, minorities and majorities conserve their character when travelling from the polarizer into the analyzer, so that for this configuration $\sigma$ does not change sign when a spin moves from one layer to the other. Further,

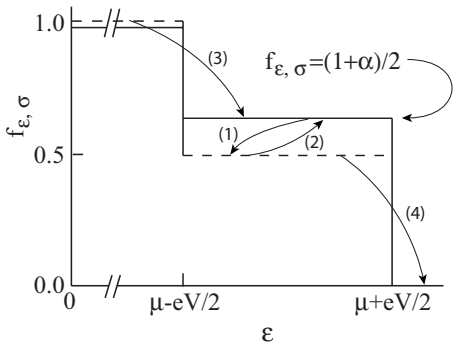


FIG. 2. Spin-dependent electron distribution $f_{\varepsilon,\sigma}$ in the analyzer. Between $\mu-eV/2$ and $\mu+eV/2$ the two levels express the spin dependence, which is absent below $\mu-eV/2$ (solid and dashed functions in that range take the value unity). For parallel (antiparallel) alignment of $\mathbf{M}_p$ and $\mathbf{M}_a$ the solid and dashed distributions correspond to majority and minority spins (minority and majority spins) in the analyzer, respectively. Arrows indicate magnon emission (process 1) and magnon absorption (processes 2, 3, 4) for antiparallel alignment. Similar processes, *mutatis mutandis*, occur for the parallel alignment.

$f_0$ is the Fermi-Dirac distribution, $\epsilon_{\mathbf{k},\sigma}$ is the total energy of an electron in state $\mathbf{k}$ and with spin $\sigma$, i.e., inclusive the electrostatic energy, and $e$ is the elementary charge $(e>0)$.

The distribution $f_{\mathbf{k},\sigma}$ is similar to that of a homogeneous diffusive $N$ point contact.[29] It is the average of two Fermi step functions displaced with respect to each other by energy eV, the difference of the chemical potentials of the electrodes. In this case, however, the weight of the functions is spin-dependent, so that two values of $f_{\mathbf{k},\sigma}$ exist for energies where $0<f_{\mathbf{k},\sigma}<1$: $f_{\mathbf{k},+1/2}=(1+\alpha)/2$ and $f_{\mathbf{k},-1/2}=1/2$. See Fig. 2. Note that in deriving Eq. (1), the effect of the analyzer on the distribution is assumed negligible. Further, we concentrate on the spin-dependent contribution of the polarizer to the electron distribution of Eq. (1), neglecting the average over the electron spins.

### B. Consistent quantum-mechanical approach to incoherent emission of nonequilibrium magnons

In the spirit of PCS of the electron-magnon interaction, the electron distribution prepared in a spin-valve point contact enables magnon emission by electrons in the analyzer, up to a maximum magnon energy $eV$. In first order, relaxation of created magnons is dominated by absorption by electrons. As usual for ferromagnets, we assume that transport is primarily due to *sp* electrons, so that these electrons control the magnon distribution, irrespective the strength of electron-magnon coupling. In this stage, we neglect escape of created magnons from the region exposed to the current and corrections to the distribution given by Eq. (1) due to magnon absorption by electrons. Thus, applying Fermi's golden rule to magnon emission and absorption, and integrating out the dependence of $f_{\mathbf{k},\sigma}$ on the directions of initial and final states (leaving only the energy and spin dependence of $f$), we find the rate equation for the occupation number of magnons $N_\omega$ with energy $\hbar\omega_{\mathbf{q}}$ in the analyzer:

$$\frac{dN_\omega}{dt} = \frac{1}{2\pi\hbar}\sum_\sigma \int d\varepsilon\, D(\varepsilon) \int d\varepsilon' D(\varepsilon')|\tilde{g}|^2 \times [f_{\varepsilon,\sigma}(1-f_{\varepsilon',-\sigma})(1+N_\omega)\delta(\varepsilon-\varepsilon'-\hbar\omega_{\mathbf{q}}) - (1-f_{\varepsilon,\sigma})f_{\varepsilon',-\sigma}N_\omega\delta(\varepsilon-\varepsilon'+\hbar\omega_{\mathbf{q}})]. \quad (2)$$

Here $D(\epsilon)$ is the electron density of states normalized with respect to the unit cell and $\tilde{g}$ is an effective matrix element for electron-magnon coupling, i.e., renormalized with respect to wave-vector nonconserving scattering. Details of this renormalization can be found in Appendix A. The sign convention of $\sigma$ in Eq. (2) is the same as in Eq. (1). The first term of the integrand applies to emission, the factor $(1+N_\omega)$ denoting the sum of spontaneous and stimulated processes. Since magnons are spin unity quanta and electron spin is conserved in magnon emission, we deal with a spin-flip process. Therefore, for antiparallel alignment of $\mathbf{M}_p$ and $\mathbf{M}_a$, the net spin of the analyzer electrons increases by unity for each magnon emitted by converting an analyzer minority spin into an analyzer majority spin. Accordingly, the first energy integration in Eq. (2) involves minority-spin electrons, while the second integration involves majority-spin electrons. For parallel alignment of the magnetizations similar reasoning applies to identify how each spin type takes part in the transitions. By nature, this magnon emission is incoherent, so that incoherent magnetization precessions result. This is in contrast to the current-induced coherent magnetization precession predicted by the spin-torque model.[1] The second term of the integrand applies to magnon absorption, in which a majority-spin electron is converted to a minority-spin electron.

For evaluation of Eq. (2) for $T=0$, where magnon creation is limited to the energy range $\hbar\omega_{\mathbf{q}} < eV$, it is helpful to recognize the possible emission and absorption processes in the analyzer. For the antiparallel alignment these are indicated in Fig. 2. Taking into account the energy range and the distribution function of the electron states involved in these processes, both for $\mathbf{M}_p$ and $\mathbf{M}_a$ parallel and antiparallel, Eq. (2) goes over into

$$\frac{dN_\omega}{dt} = -\frac{1}{\tau_{m-e}}\left[N_\omega\left(1+\frac{eV}{\hbar\omega_{\mathbf{q}}}S_z\right) - \frac{eV-\hbar\omega_{\mathbf{q}}}{4\hbar\omega_{\mathbf{q}}}(1-2S_z)\right]. \quad (3)$$

Here $S_z = \alpha(\mathbf{M}_a\cdot\mathbf{M}_p/2M_aM_p)$ is a projection of $\mathbf{M}_a$ on $\mathbf{M}_p$, weighed by the current polarization. Whereas the spin polarization is defined with respect to $\mathbf{M}_p$, $S_z$ takes into account the sensitivity of magnon-electron processes to the polarization with respect to the direction of $\mathbf{M}_a$. In Eq. (3) $\tau_{m-e}^{-1} \approx \hbar^{-1}|\tilde{g}|^2[D(\epsilon_F)]^2\hbar\omega_{\mathbf{q}}$ is the inverse of the characteristic time for magnon-electron processes.

Equations (2) and (3) describe transfer of spin from the spin-polarized current to the magnon system. Due to this transfer the population of nonequilibrium magnons increases until a steady state is reached where magnon emission and absorption balance each other, i.e., where $dN_\omega/dt=0$. For magnons of energy $\hbar\omega_{\mathbf{q}}$ the steady state is characterized by an effective magnon temperature $T_{m,\omega}^{\text{eff}}$, obtained by equating the number of such magnons to the average population as given by the Planck distribution ($k_B$ is Boltzmann's constant):

$$T_{m,\omega}^{\text{eff}} = \frac{1}{k_B}\frac{eV-\hbar\omega_{\mathbf{q}}}{4}\frac{1-2S_z}{1+(eV/\hbar\omega_{\mathbf{q}})S_z}. \quad (4)$$

In the limit of weak polarization and for magnon energies $\hbar\omega_{\mathbf{q}} \ll eV$ one obtains $T_{m,\omega}^{\text{eff}} \approx eV/4k_B$. The effective temperature is larger for $S_z<0$ (antiparallel configuration) than for $S_z>0$ (parallel configuration). This is natural, because the phase volume for magnon creation processes is larger when $S_z<0$. Moreover, in the antiparallel configuration ($S_z<0$), $T_{m,\omega}^{\text{eff}}$ diverges at a critical voltage given by

$$V_c = -\frac{\hbar\omega_{\mathbf{q}}}{eS_z}. \quad (5)$$

This is interpreted as an unlimited increase of the magnon population, resembling a magnon avalanche. This highly excited state of the analyzer goes along with a strongly suppressed magnetization and may lead to critical behavior similar to the phase transition to the normal state at the Curie temperature, which results from strong *thermal* excitation of magnons. As seen in Eq. (3), $dN_\omega/dt$ is positive at voltages exceeding $V_c$, so that $N_\omega$ has a positive increment in this range. Note that in the discussion given above the positive sign of $V$ corresponds to the polarity of the bias voltage as in Fig. 1. For the opposite sign of $V$ the antiparallel configuration is stable, while the instability takes place for the parallel configuration.

To further discuss this critical behavior, we introduce the magnon concentration $n_m$ ($n_m \leq 1$) normalized with respect to the volume $a^3$ of the elementary cell:

$$n_m = \frac{a^3}{\Omega}\int N_\omega \nu_m(\omega) d\omega.$$

Here $\nu_m(\omega)$ is the magnon density of states and $\Omega$ is the normalizing volume. The maximum $n_m=1$ corresponds to complete suppression of magnetization. Note that a decrease of the magnetization $|\mathbf{M}|$ of a ferromagnet with an increase of $n_m$ for small $n_m$ is a well-established behavior, which in particular applies to the decrease of $|\mathbf{M}|$ with increasing temperature. This behavior is interpreted as an uncertainty in the orientation of $\mathbf{M}$ by an angle $\theta$ ($\theta^2/2 \sim n_m$) with respect to its orientation in saturation (where $n_m=0$). To our knowledge the situation of very high magnon occupation numbers ($n_m \sim 1$) so far did not receive proper theoretical treatment. We may only speculate that the above-mentioned magnon avalanche, tending to suppress the average magnetization when $n_m \sim 1$, finally leads to a "switching," that is to formation of a stable magnetic state of the analyzer with a direction of $\mathbf{M}_a$ opposite to its initial direction. Indeed, the sign of $S_z$ reverses from negative to positive as a result of this switching, leading to stabilization. However, before the system comes to switching, one expects that $n_m$ can stabilize at some $n_m \ll 1$ due to mechanisms not included in Eq. (2). Candidate mechanisms are the electron-magnon and the magnon-magnon interaction, ingredients of magnon kinetics at large magnon occupation numbers (but still in the regime of con-

ventional magnon theory, where $n_m \ll 1$). The role of electron-magnon processes is discussed below, while the magnon-magnon interaction is the subject of Sec. III.

In case of high enough magnon occupation numbers, electron-magnon processes can modify the electron distribution function with respect to Eq. (1). Then, the stimulated magnon-emission rate becomes so high that it may lead to decay of the spin-dependent electron distribution in the analyzer. Magnon emission related to the nonequilibrium spin distribution is principally restricted by the magnitude of the spin-current density $j_{s,\mathrm{inj}}$ injected into the analyzer. Thus, with increasing $j_{s,\mathrm{inj}}$ a crossover can be effected from the voltage-controlled regime, where Eq. (1) holds, to a current-controlled regime, where the approximation leading to Eq. (1) breaks down due to strong magnon emission. To estimate the critical concentration $n_{m,c}$ at the crossover we use the rate equation

$$\left(\frac{dn_m}{dt}\right) = \left(\frac{dn_m}{dt}\right)_{\mathrm{emission}} + \left(\frac{dn_m}{dt}\right)_{\mathrm{decay}}, \tag{6}$$

which is obtained by integrating Eq. (3) over the magnon phase volume. The emission term, which results from the terms $\propto eV$ in Eq. (3), describes magnon emission by nonequilibrium electrons. The decay term, which even in equilibrium is nonzero, describes magnon absorption by electrons. When Eq. (1) holds, the decay term is given by

$$\left(\frac{dn_m}{dt}\right)_{\mathrm{decay}} = -\frac{1}{\tau_{m-e}} n_m, \tag{7}$$

while the emission term is equal to

$$\left(\frac{dn_m}{dt}\right)_{\mathrm{emission}} = \frac{eV|S_z|}{\hbar\omega\tau_{m-e}} n_m. \tag{8}$$

According to the considerations given above the emission term is restricted at the level

$$j_{s,\mathrm{inj}} \frac{a^3}{t_a}. \tag{9}$$

Thus one concludes that for $V$ only slightly above the threshold value $V_c$ (where the critical value of the $j_{s,\mathrm{inj}}$ is written as $j^c_{s,\mathrm{inj}}$) the crossover from the bias-controlled regime to the current-controlled regime takes place at

$$n_{m,c} = \tau_{m-e} j^c_{s,\mathrm{inj}} \frac{a^3}{t_a}. \tag{10}$$

In the voltage-controlled regime $\tau_{m-e} = k_F l_a / \omega$ (see Appendix A), while $j_{s,\mathrm{inj}} \sim \eta S_z e V v_F D(\epsilon_F)$, where $D(\epsilon_F) \sim a^{-3}\epsilon_F^{-1}$ and $\eta = j_{s,\mathrm{inj}} / j^{\mathrm{ball}}_{s,\mathrm{inj}} \ll 1$. Thus one obtains $n_{m,c} \sim \eta_c$. Here $j^{\mathrm{ball}}_{s,\mathrm{inj}}$ is the injected spin-current density which would exist under the same bias voltage in a ballistic structure. Note that until now we have taken into account only electron-magnon processes.

Having in mind Eq. (6) and the restriction of the emission term, one would expect that the magnon-electron processes stabilize the magnon occupation for the current-controlled regime at the level ($V \leq V_c$)

$$n_m = n_{m,c} \frac{V}{V_c}. \tag{11}$$

This, however, would imply that magnon decay processes still follow the estimates of Eq. (7) relevant for the voltage-controlled regime, implying that Eq. (1) holds. At the same time, as shown in Appendix B, large magnon occupation numbers also lead to saturation of the magnon decay efficiency. This saturation arises from the bottleneck represented by the finite electron diffusion current from the analyzer. Further, the estimates given in Appendix B imply that

$$\left(\frac{dn_m}{dt}\right)_{\mathrm{decay}} \leq \frac{1}{\tau_{m-e}} n_{m,c} = \frac{1}{\tau_{m-e}} \eta_c. \tag{12}$$

Thus it appears that in the current-controlled regime both spin pumping and spin decay in the analyzer are restricted by the electron diffusivity and that the magnetization evolution cannot be stabilized unless the threshold value of the bias voltage is reached.

Now let us discuss the spectrum of the excited magnons. In principle, the only limitation is given by the condition $\hbar\omega < |eVS_z|$. Having in mind that for the point-contact geometry voltages as high as at least several tens of mV are accessible, one concludes that magnon energies of at least 10 mV are possible. From the quadratic spectrum of the magnons one concludes that the corresponding magnon wavelength is of the order of 1 nm. Although magnons with smaller frequencies have faster exponential evolution [see Eq. (8)], the magnon-magnon processes considered in the following section can shift the distribution to higher frequencies.

To conclude this section, in the voltage-controlled regime the magnetization evolution of the analyzer does not affect the local nonequilibrium spin accumulation and it is this voltage-dependent spin accumulation which controls the evolution. For ballistic structures this holds up to $n_m \sim 1$ or to precession angles $\theta$ close to unity. In the current-controlled regime the accumulation depends on the magnetic evolution in the analyzer and it is the spin current which supports the evolution.

## III. STABILIZATION BY MAGNON-MAGNON PROCESSES

### A. Introduction to three- and four-magnon processes

Magnon-magnon processes are a precursor of the general nonlinearity of magnon physics at high magnon occupation levels. One distinguishes between three-magnon processes, which originate from the dipole-dipole interaction and are spin nonconserving, and four-magnon processes, which arise from the exchange interaction and conserve both total spin and the number of magnons.[30]

In a four-magnon process $(1,2 \rightarrow 3,4)$ two incoming magnons are annihilated while scattering at each other, to form two new, outgoing magnons. The occurrence rate of this process for a given incoming mode 1 is[30]

$$\frac{1}{\tau_4} \propto \gamma_4 N_{\omega_2}(1+N_{\omega_3})(1+N_{\omega_4}), \tag{13}$$

where $\gamma_4$ is a dimensionless parameter, which for a 3D spectrum and for participating wave vectors of similar magnitude $q$ equals $(qa)^8$. Since four-magnon processes conserve both the number of magnons and the energy, they cannot efficiently modify the magnon distribution if it is initially concentrated at the lowest possible energies. Thus four-magnon processes cannot stabilize $n_m$ and therefore are ineffective in preventing the magnon avalanche in the analyzer.

A three-magnon process $(1,2\rightarrow 3)$ is the coalescence of magnon modes 1 and 2 into a magnon mode 3. This process can redistribute the magnon occupation to higher energies. The occurrence rate of this process for a given incoming mode 1 is[30]

$$\frac{1}{\tau_3} \sim \frac{2\pi}{\hbar}\frac{(\mu_B M)^2}{k_B\Theta_C}\gamma_3 N_{\omega_2}(N_{\omega_3}+1). \tag{14}$$

Here $\Theta_C$ is the Curie temperature, $M$ is the magnetization, while $\gamma_3(1,2)$ is a dimensionless parameter resulting from the summation over available modes (2, 3) and depending on the magnon spectrum and on momentum conservation. For a 3D magnon spectrum and large magnon wave vectors one has $\gamma_3 \sim q_2 a$, where $q_2$ is the wave vector of mode 2. For small $q$, if $\omega(q\rightarrow 0)$ is isotropic in $\mathbf{q}$ space, momentum conservation restricts coalescence processes to $\omega_3$ values with $\omega_3 > 3\omega(q\rightarrow 0)$.

In the thin analyzer, however, momentum conservation in a three-magnon process does not necessarily hold, due to arguments similar to those presented in Appendix A. Applying the approach of Appendix A to three-magnon processes in the limit of weak magnon-magnon scattering, one obtains the estimate

$$\gamma_3 \propto (q_3 l_{m,3})^{-1}\nu_m(\omega_3), \tag{15}$$

where $l_{m,3}$ is the magnon mean free path for the mode 3. Thus momentum nonconserving three-magnon processes can be effective in modifying the critical behavior if the spatial scale of the scatterer distribution is comparable with the magnon wavelength. Consequently, for this situation a relaxation-time term based on $\tau_3$ should be added to Eq. (2), to describe either a decrease or increase of $N_\omega$. To do so, it is helpful to write the occupation number $N_\omega$ in terms of the normalized parameter $n_{m,\omega}$ as

$$N_\omega \sim n_{m,\omega}\mathcal{V}_\omega^{-1}, \tag{16}$$

where $\mathcal{V}_\omega$ is the relative phase volume for the corresponding modes [for a 3D magnon spectrum $\mathcal{V}_\omega \sim (qa)^3$]. So, in spite of the weakness of the dipole-dipole interaction, three-magnon processes can be relevant at small wave vectors, since the smallness can be compensated by a large factor $\mathcal{V}_\omega^{-1}$, even at $n_{m,\omega} < 1$.

### B. Three-magnon processes at low rate: $N_3 \ll 1$

We first suppose that the number of emitted magnons $N_3$ is small, so that stimulated coalescence can be neglected. Equation (3) is then rewritten as $(\omega_1=\omega_2=\omega$; for simplicity dropping the index $q$ of $\omega$ and the index $\omega$ of $n_{m,\omega})$

$$\frac{dN_\omega}{dt} = -\frac{1}{\hbar\omega\tau_{m-e}}(S_z eV+\hbar\omega)N_\omega - \frac{2\pi}{\hbar}\frac{(\mu_B M)^2}{k_B\Theta_C}n_m\frac{\gamma_3}{\mathcal{V}_\omega}N_\omega. \tag{17}$$

As a result magnon emission is stabilized at magnon concentration

$$\tilde{n}_m = \frac{k_B\Theta_C}{2\pi(\mu_B M)^2\omega\tau_{m-e}}\frac{\mathcal{V}_\omega}{\gamma_3}(|S_z|eV-\hbar\omega). \tag{18}$$

Clearly, three-magnon processes provide for a gradual evolution of $\tilde{n}_m$ with increasing $V$ above $V_c=\hbar\omega/|S_z|e$, followed by reversal of the magnetization at some $V=V_{c1}$ corresponding to $\tilde{n}_m(V)\sim 1$. To estimate the range for this behavior, one notes that for typical ferromagnets $k_B\Theta_C/2\pi\mu_B M \sim 10^3$. Further, from the estimate in Appendix A it follows that $\omega\tau_{m-e} \sim 10-100$. Thus, also assuming $\mathcal{V}_\omega/\gamma_3 \sim 10^{-2}$, one obtains

$$\tilde{n}_m \sim (10^{-3}-10^{-2})\frac{(|S_z|eV-\hbar\omega)}{\mu_B M},$$

where $\mu_B M \sim 0.01$ meV. Thus the values $n_m < 1$ are still expected even for $|V-V_c| \sim 1$ mV. However, for small values of $\gamma_3$ it may occur that $V_{c1}$ is very close to $V_c$, so that an appreciable region of gradual evolution does not exist. (See discussion below.)

### C. Three-magnon processes at high rate: confluence to mode $\omega_3$, leading to stimulated emission of this mode

Now we consider large occupation numbers $N_3$, which leads to stimulated emission of the corresponding magnons. For the mode $\omega_3$ one has $(\omega_1=\omega_2=\omega)$

$$\frac{dN_{\omega_3}}{dt} = -\frac{1}{\hbar\omega_3\tau_{m-e}}\left[(S_z eV+\hbar\omega_3)N_{\omega_3} - \frac{eV-\hbar\omega_3}{4\hbar\omega_3}(1-2S_z)\right] + \frac{2\pi}{\hbar}\frac{(\mu_B M)^2}{k_B\Theta_C}\times\frac{\gamma_3}{\mathcal{V}_\omega^2}n_m^2(N_{\omega_3}+1). \tag{19}$$

We assume that, since $\omega_3$ is at least twice as large as $\omega_1$, $S_z eV+\hbar\omega_3 > 0$. So, in a stationary situation one has

$$N_{\omega_3} \sim \frac{n_m^2+\beta}{n_c^2-n_m^2}, \tag{20}$$

where

$$n_c^2 = \frac{k_B\Theta_C}{2\pi(\mu_B M)^2\omega_3\tau_{m-e}}\frac{\mathcal{V}_\omega^2}{\gamma_3}(S_z eV+\hbar\omega_3), \tag{21}$$

while

$$\beta = \frac{k_B\Theta_C}{2\pi(\mu_B M)^2\omega_3\tau_{m-e}}\frac{\mathcal{V}_\omega^2}{\gamma_3}\frac{(eV-\hbar\omega_3)(1-2S_z)}{4}. \tag{22}$$

In this limit of large $N_3$ the stationary solution for $N_\omega$ (denoted by the normalized concentration $\tilde{\tilde{n}}_m$) then follows from

$$\tilde{n}_m = \tilde{\tilde{n}}_m + \frac{\tilde{\tilde{n}}_m^3 + \beta \tilde{\tilde{n}}_m}{n_c^2 - \tilde{\tilde{n}}_m^2}, \tag{23}$$

where $\tilde{n}_m$ is given by Eq. (18). As seen, the solution of this equation depends on the ratio

$$\frac{n_c}{\tilde{n}_m} \sim N_{\omega_3}^{-1} \sim \left[\frac{2\pi(\mu_B M)^2 \omega \tau_{m-e} \gamma_3}{k_B \Theta_C}\right]^{1/2} \frac{(S_z eV + \hbar\omega_3)^{1/2}}{|S_z| eV - \hbar\omega}, \tag{24}$$

which defines two limiting scenarios. In the first scenario, determined by $\tilde{n}_m \ll n_c$, the stationary solution is

$$\tilde{\tilde{n}}_m \sim \tilde{n}_m, \tag{25}$$

so that the condition for gradual evolution is the same as for $\tilde{n}_m$. In the second scenario $\tilde{n}_m \gg n_c$ one has

$$\tilde{\tilde{n}}_m \sim n_c. \tag{26}$$

So, three critical voltages $V_c$, $V_{c1}$ and $V_{c2}$ can be distinguished. With $V$ increasing above $V_c$ (but $\tilde{n}_m \ll n_c$) one first has $\tilde{\tilde{n}}_m \sim \tilde{n}_m$, while above some $V_{c2}$ the condition $\tilde{n}_m > n_c$ can be reached (provided $V_{c2} < V_{c1}$), so that $\tilde{\tilde{n}}_m \sim n_c$. It should be noted that for $\tilde{\tilde{n}}_m \sim n_c$ the value of $\tilde{\tilde{n}}_m$ *decreases* with increasing of $V$, since the magnon emission corresponds to $S_z eV < 0$.

Thus a nonmonotonous evolution of the magnetization is expected: At critical bias $S_z eV_c = -\hbar\omega$ the value of $n_m = n_c(V = V_c)$ is reached, while a further increase of $V$ leads to a decrease of the magnons concentration. In this regime one has

$$N_{\omega_3} \sim \frac{\tilde{n}_m}{n_c},$$

so that $N_{\omega_3}$ increases with increasing $V$.

According to the considerations given above, this approximation holds only up to the biases $V = 2V_c$, where the mode $\omega_3$ starts to be critical. A further increase of the magnon concentration is expected to support multimagnon processes of both spin-conserving (exchange) and spin nonconserving (dipole-dipole) types involving more than three and four magnons, respectively. These processes put to the stage other modes with frequencies higher than $\omega_3$ which at biases $V = 2V_c$ are still not critical and which support spin decay due to magnon-electron processes. The quantitative analysis of the corresponding energy diffusion, which should be made carefully and with an account of the dynamics of all modes involved, will not be discussed here further.

It is instructive to estimate the critical bias $V_{c2}$. Using $|S_z| \simeq 1$, $eV_c \simeq \hbar\omega$ and $S_z eV_{c2} + \hbar\omega_3 \simeq \hbar\omega$ one obtains

$$\frac{V_{c2} - V_c}{V_c} \simeq \left(\frac{\mu_B M}{k_B \theta_C}\right)^{1/2} \left(\frac{\mu_B M}{\hbar\omega}\right)^{1/2} (\omega \tau_{m-e} \gamma_3)^{1/2}. \tag{27}$$

The magnon frequency $\omega$ increases with increasing magnetic field, which is due to the field dependence of the magnon dispersion: $\omega = \omega_0(H) + Cq^2$. As a result, the wave vector of mode 3 also increases with increasing $\omega_0$ since $\omega_1 \sim \omega_0$, $\omega_3 = \omega_0 + Cq_3^2 \sim 2\omega_0$. According to Eq. (15) $\gamma_3 \propto q_3^{-1} \nu_m(\omega_3)$ provided $l_m$ is controlled by the lattice disorder of the crystalline layer and does not depend on $q_3$. For a bulk 3D spectrum one has $\nu(\omega_3) \propto \omega_3^{1/2}$, while for a 2D spectrum $\nu_m = \text{const}$. As a result Eq. (27) implies that the bias region of gradual evolution according to the second scenario strongly decreases with increasing field. For 3D magnons (generated at large enough biases) the width of this region decreases as $\propto H^{-1}$. This leads to a steplike increase of $n_m$ just above the critical bias $V_c$. This step can be seen as a spike in the differential magnetoresistance. The behavior of the system according to these considerations is schematically depicted in the phase diagram of in Fig. 3.

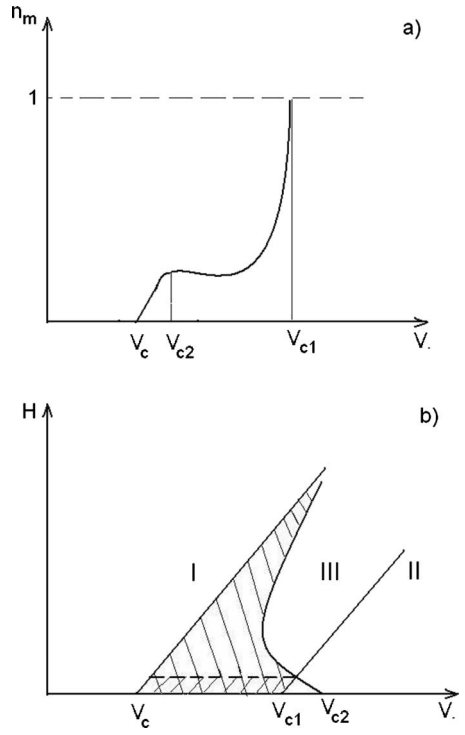


FIG. 3. (a) Dependence of $n_m(V)$ for a given magnetic field $H$ in the situation $V_{c2} < V_{c1}$. (b) Phase diagram of the magnetization evolution given by curves $V_c(H)$, $V_{c1}(H)$, and $V_{c2}(H)$ under the assumption $V_{c1}(0) < V_{c2}(0)$. According to the considerations given in the text, $V_{c1} \propto H$, $V_c \propto H$ while $(V_{c2} - V_c) \propto H^{-1}$. Region I is the phase of antiparallel magnetizations of the layers. Region II is the phase of parallel magnetizations. Region III corresponds to a crossover from the quantum (magnon) scenario to the torque scenario. Shaded region corresponds to the spikelike regime. Doubly shaded region corresponds to the hysteretic regime.

We note that a more detailed picture including magnon-magnon processes is rather complex and sensitive to all kinds of details such as the magnon spectrum. Our minimal model only aims to qualitatively reveal the main features. In spite of this restriction, it is concluded that magnon-magnon processes lead to saturation of magnon emission at $n_m < 1$, the region where no switching occurs. As a result, gradual evolution of the magnetization with increasing bias is possible. The scenario depends on the relation between $n_c$ and $\tilde{n}_m$ as well as on the value $n_c$. A more quantitative analysis should be based on estimates of parameters such as $\gamma_3$ and $\mathcal{V}_\omega$, which is beyond the present scope.

## IV. COMPARISON TO PREVIOUS THEORETICAL APPROACHES

Here, the present theory is compared with the approaches of Slonczewski,[1] Berger,[2] and Tserkovnyak *et al.*,[22–24] restricting ourselves to the most salient points. In Ref. 1 spin transfer from the incident electrons to the layer is proportional to the amplitude of magnetization precession. Spin transfer is zero for $\mathbf{M}_p$ parallel or antiparallel to $\mathbf{M}_a$, while in our approach spontaneous magnon emission also exists in these special cases, allowing spin relaxation. In Ref. 1 the spin transfer from the incident electrons is equal to $j_{s,\mathrm{inj}} \sin\theta$, provided $t_a > l_p \sim (1/k_F)\varepsilon_F/E_{\mathrm{ex}}$. Here $E_{\mathrm{ex}}$ is the exchange energy, $l_p$ is the spin precession length, and $j_{s,\mathrm{inj}}$ is the spin-current density injected into the analyzer. Since $E_{\mathrm{ex}}$ is not too small with respect to the Fermi energy, this condition holds for practical values of $t_a$. Thus the mechanism of Ref. 1 is restricted to the near-surface layer of thickness $l_p$.

The evolution of the precession angle is described by Eq. (17) of Ref. 1, the key equation of this paper, which in our notation reads

$$\frac{d\theta}{dt} = -\left(\alpha_0\omega - \frac{j_{s,\mathrm{inj}}a^3}{t_a}\right)\sin\theta. \tag{28}$$

Here $\alpha_0$ is the Gilbert damping parameter. To compare with our results, we first take into account that for small $\theta$ the number $n_m$ of coherently excited magnons is related to $\theta$ as $n_m \sim \theta^2/2$. Then, we identify the product $\alpha_0\omega$ with the magnon relaxation rate $1/\tau_m$. Thus, Eq. (28) is rewritten as

$$\frac{dn_m}{dt} = \left(\frac{j_{s,\mathrm{inj}}a^3}{t_a} - \frac{1}{\tau_m}\right)n_m. \tag{29}$$

Note that for magnetization configurations close to collinear this equation is also similar to the ones considered in paper,[24] aimed to generalize the ideas of Slonczewski and Berger with an account of an electronic mechanism of Gilbert damping.[23] A comparison of Eq. (29) to our results leads to the following considerations and conclusions.

(1) Equation (29) indicates that the spin-torque approach deals with a spin-current controlled situation. Thus this approach is incapable to handle relative magnetization orientations of polarizer and analyzer close to collinear, for which the voltage-controlled regime developed in this article does predict a proper magnetization evolution. Further, it should be noted that in contrast to our picture, where in the current-controlled regime the rate of magnetization change is saturated—see Eqs. (8) and (9)—here one still deals with an exponential behavior.

(2) By relating the magnon relaxation rate $1/\tau_m$ to the finite electron diffusivity discussed at the end of Sec. II and in Ref. 23, one can make the identification $1/\tau_m \simeq \eta/\tau_{m-e}$. It then follows that the threshold for switching $V_c$ of the spin-torque approach is identical to the one we have obtained (provided only electron-magnon processes are taken into account). Indeed, if one inserts into Eq. (29) $\tau_m^{-1} = (j_{s,\mathrm{inj}}/j_{s,\mathrm{inj}}^{\mathrm{ball}})\omega/(k_F t_a)$ (according to our estimate of $\tau_{m-e}$) and $j_{s,\mathrm{inj}}^{\mathrm{ball}} \sim S_z eVD(\epsilon_F)v_F$, one immediately obtains the critical voltage $V_c = \hbar\omega/eS_z$, in agreement with our Eq. (5). This means that the evolution of the analyzer magnetization, if started according to our scenario from a collinear orientation, can in principle crossover to the spin-torque scenario at large $n_m$ or, correspondingly, at large precession angles $\theta$.

(3) Nevertheless, the rate of magnetization evolution in our magnon model is faster than predicted by the spin-torque model until $n_m \sim 1$ [compare Eqs. (6), (7), (9), and (29)]. That is, at least in the range $\theta \ll 1$ our model holds and allows faster magnetization evolution than the spin-torque model. Only at $\theta \sim 1$ (when magnons are not well defined) the classical spin torque model appears to be relevant.

This discrepancy between the physical pictures discussed above must of course relate to a difference of the two approaches. Our approach is completely quantum-mechanical and consistent, while the approach in Ref. 1 combines a quantum-mechanical treatment of the electron-spin evolution with a semiclassical transfer of the $x$ component of the spin to the layer, using the classical Landau-Lifshitz equation. As a result, in Ref. 1 some problems are not unequivocally treated, in particular the mechanism leading to a change of the $z$ component of the spin in units $\frac{1}{2}\hbar$. It is this change, as we demonstrate above, that governs spin evolution in a consistent quantum-mechanical picture and that leads to incoherent behavior. Further, in Ref. 1 it is unclear how the spin of a single electron is transferred to the layer as a whole, since in semiclassical spin transfer an electron is only coupled to its closest surrounding.

These questions were partially noted by Berger,[2] who exploits a mechanism of boundary-induced spin-wave emission with similarities to that of Ref. 1. Berger treats transfer of the $z$ component of the electron spin by just postulating a simple relaxation time approximation to satisfy the required quantized change of the electron spin. [Eqs. (9)–(12) in Ref. 2.] He concludes that the spin-wave system is unstable beyond some critical current, opposed to our finding that instability of the magnon system sets in beyond a critical voltage. However, just like in Ref. 1, Berger neglects the nonequilibrium electron distribution as well as spin accumulation produced by the polarizer, which even exist in the absence of the analyzer. In other words neither Berger nor Slonczewski produce a voltage-controlled regime. Instead, Berger relates the chemical potential difference of the majority and minority subbands to a difference in pumping of electron momenta at the boundary due to different drift currents [Eq. (22) of Ref. 2]. In our opinion this is equivalent to the assumption that the spin (or energy) diffusion length equals the elastic mean free path, which strongly underestimates the real potential difference for diffusive devices where it is controlled by the applied bias.

In Ref. 24 Tserkovnyak *et al.* generalize the approaches of Refs. 1 and 2 on the basis of their earlier estimate[23] of the electronic contribution to Gilbert damping. Note that, in contrast to our result that electronic damping occurs in the bulk of the ferromagnet (analyzer), the authors of Ref. 23 relate it to escape of the electrons to the normal region. Again, it reflects that Refs. 23 and 24 are concerned with the current-controlled regime, which is the essence of the spin-torque approach.

As shown in Appendix A, coupling between electrons and magnons in the ballistic case is controlled by the finite thickness effect, yielding a coupling efficiency $\propto t_a^{-1}$. This result

coincides with the prediction in Ref. 23, although formally the physics is different. Indeed, in our case the same result would even be obtained for an isolated ferromagnet with an equilibrium electron distribution. While this applies to slight deviations of the magnon distribution from its equilibrium value, it breaks down for intensive spin pumping from magnetic degrees of freedom to the electrons. As shown in Appendix B, the equilibrium electron distribution can hold only if polarized electrons escape the ferromagnet or if spin flips occur in it. This agrees with Ref. 22. However, from Appendix A, we know that the electron-magnon coupling in diffusive ferromagnetic layers acquires a bulk character which lifts the dependence of the electron-magnon matrix element on the layer thickness. We believe this can explain the disagreement between different experimental results mentioned in Ref. 22. It is important to note that electron escape from the ferromagnet can still maintain the electron distribution in equilibrium provided the resistance introduced by the ferromagnetic layer is less than the resistance of the normal part at distances of the order of spin diffusion length.

Here we would like to also mention the approach considered in Ref. 31 (see also Ref. 32), where the nonequilibrium spin population in spin valves is analyzed. The analysis is made for the spin-current controlled regime, while the nonequilibrium spin distribution is only considered for the normal layers, aiming for an account of spin-flip processes. The presence of the ferromagnetic layers is accounted for by using proper boundary conditions, similar to those in Refs. 23 and 24, while the dynamics of the ferromagnets is described by the classical Landau-Lifshitz equations. Further, the papers in Refs. 33 and 34 report theoretical studies of current-induced excitation of magnetization precession. However, again, these studies are based on the Landau-Lifshitz equations and are in the framework of the spin-torque picture.

To conclude this section, we note that for high excitation levels violating the condition $n_m \ll 1$ there is the crucial question whether the magnetization evolution follows our incoherent scenario or the coherent classical scenario considered in Ref. 1 (with a Gilbert damping parameter corrected for the nonequilibrium electron distribution). In any case the initial evolution will follow our scenario if the system starts from $\mathbf{M}_p$ and $\mathbf{M}_a$ being parallel or antiparallel. The reason is that our scenario is based on magnon excitations, which can be considered as quantum fluctuations. These even exist for $\theta=0,\pi$. The further behavior is not completely clear since, as noted above, the situation of very high magnon occupation numbers requires further analysis. In particular, one can expect a kind of production of coherency originating from effective magnon-magnon processes (presumably four-magnon processes, which we have not taken into account within our simplified picture), thus establishing coherent evolution. Note that a similar problem was discussed for acousto-electric generators of sound waves, where a coherent signal arose from initial electron-drift driven emission of incoherent phonons.[35]

## V. COMPARISON TO EXPERIMENTAL SITUATION

Thus a magnon avalanche triggered by incoherent stimulated emission of magnons determines the magnetization evolution at bias voltages smaller than the critical voltage for magnetization switching predicted in Ref. 1. Further evolution at these moderate biases is characterized by a very high magnon temperature, while nevertheless the initial magnetization direction is maintained. This is unlike the switching predicted in Ref. 1. In our scenario an initial steplike behavior of the magnetization at $V_c=|\hbar\omega_q/eS_z|$ can be followed by a gradual increase of the magnon population and, correspondingly, by a gradual decrease of the magnetization.

The gradual evolution of the resistance and thus of the magnetization is regularly observed.[3–6,39] In many cases this behavior has a threshold character and is observed only for one of the magnetic configurations of the system. In Refs. 3 and 5 the gradual evolution is ascribed to an increase of the electron scattering at equilibrium phonons and magnons with increasing current. We agree on the argument of increasing electron-magnon scattering, but do not believe that the increase results from simple heating, as implied by the cited authors. Instead, we believe that this behavior arises from electron scattering at nonequilibrium magnons, which are excited to high occupation numbers, which are subsequently stabilized according to the scenarios discussed above.

References 3 and 5 also report on current-induced magnetization switching. The switching is hysteretic as a function of current and external magnetic field and is interpreted in terms of the spin-torque theory.[1] At high magnetic fields and for one current direction spikes are observed instead of switching, which is attributed to emission of spin waves. Since the theory[1] exploits a constant Gilbert damping parameter and therefore cannot describe a stable spin-precessing mode, the authors of Ref. 5 need to invoke a precession-angle dependent damping parameter. This can explain the spikes but not the gradual evolution clearly present in the traces. The transition from hysteretic to the spikelike behavior with increasing magnetic field is also reported in Ref. 9 for small permalloy spin valves. In this work qualitative arguments involving magnetic excitations (magnons) and a resulting effective temperature exceeding the bath temperature are used to explain the observed behavior. In the vicinity of the spike they also observe random telegraph noise involving two resistance levels. This noise is pronounced only in a very narrow bias region and shows no hysteresis. This cannot be explained by magnetization reversal since the anisotropy field required for this should give rise to hysteresis.

To understand the mechanism of such spikes and two-level fluctuations in the framework of our model, let us take into account that the resistance of the ferromagnetic layer increases due to a contribution of electron-magnon processes. Denoting the zero bias resistance of the device as $R_0$, we write

$$R = R_0 + An_m, \tag{30}$$

where for simplicity we assumed that the additional resistance is simply proportional to the number of excited magnons. In regime 1 considered in Sec. III we have

$$n_m = B(V - V_C)\theta(V - V_c),$$

where the coefficient $B$ is given by Eq. (18) and the $\theta$ function describes the threshold character of the behavior. Taking

into account that the additional resistance is much less than $R_0$, we obtain for the differential conductance

$$\frac{\partial I}{\partial V} = \frac{1}{R_0} - \frac{AB}{R_0^2}(2V - V_c)\theta(V - V_c). \tag{31}$$

This differential conductance becomes *negative* for $V > V_c$ provided the product $AB$ is large enough. It stays negative up to $V = V_{c1}$, where the layer switches and the differential conductance is positive (scenario 1 of Sec. III) or up to $V = V_{c2}$ where the magnon population is stabilized and the differential conductance is positive as well (scenario 2 of Sec. III). The behavior in either scenario corresponds to an $N$-shaped $I$-$V$ curve. In nanostructures such an $I$-$V$ curve can lead to random telegraph noise,[37] as a result of fluctuations of the system parameters. We deal with a system strongly out of equilibrium, for which the corresponding fluctuations can exist even at zero bath temperature. In particular, if the electron distribution is given by Eq. (1), the bias $eV$ plays the role of an effective temperature. A quantitative analysis of the fluctuations related to the nonequilibrium magnons needs a consistent analysis of four-magnon processes. This goes beyond the present article. Here we emphasize that random telegraph noise does not necessarily arise from activation over some "magnetic" barrier, as assumed in Refs. 9 and 10. However, we agree with the assumptions in Refs. 4 and 9 that the noise can arise from fluctuations in the nonequilibrium magnon system and can exist at low bath temperature.

In reviewing these experimental papers, we are pointed to the coexistence of the gradual behavior followed by switching behavior, gradual behavior followed by spikelike behavior and random telegraph noise at low temperature. This coexistence and the theoretical paper[37] strongly suggest that our model of nonequilibrium magnon emission, since it can account for the phenomena mentioned, is a major ingredient in their explanation.

Now let us discuss to what extent we deal with coherent or incoherent processes. A recent paper[16] reports a time-domain study of the nonequilibrium nanomagnet dynamics, in particular an oscillatory voltage generated by the magnetization precession. Based on this observation the authors of Ref. 16 state that the measurements are not consistent with models in which the dominant spin-transfer mechanism is incoherent magnon excitation equivalent to effective heating. The first thing to note is that incoherent magnon excitation is not necessarily equivalent to effective heating. Further, the measured coherency cannot be absolute, since it will be subject to an effective frequency width $\delta\omega \approx t^{-1}$ (where $t$ is the observation time). This means that any signal to some extent is incoherent. When a periodic signal is observed, it only means that $\delta\omega \ll \omega$. As for our model, there are several factors that tend to establish a degree of coherency, even when starting from the purely incoherent processes described by Eq. (2), the rate equation for the magnon occupation number. The first factor, which exists in a purely linear picture and was already mentioned in Ref. 2, is that the exponential increase of the magnon occupation in time leads to narrowing of the frequency distribution around the frequency related to maximal increment. Another factor results from the nonlinearity of the dynamics with respect to the magnon occupation numbers. As we mentioned in Sec. IV, one expects that four-magnon processes can lead to Bose condensation of magnons at the lowest energy levels available, leading to a decrease of $\delta\omega$. Then, we would like to emphasize once more that in our picture we deal with relatively small magnon numbers ($n_m \ll 1$), so that indeed a description in terms of magnons is justified. As it was mentioned above, at larger occupation numbers the nonlinearity of the magnon dynamics can result in a purely classical picture of precession.

Finally, let us turn to the problem of coexistence of the quantum (magnon) evolution of the magnetization and the semiclassical evolution from another point of view. For simplicity, we restrict ourselves to the case of high external magnetic fields $H > H_a$, where $H_a$ is an anisotropy field. Thus at the equilibrium we have $\mathbf{M}_a \| \mathbf{H}$. Now let us assume that the bias is applied to the structure such as $eVS_z < 0$. As a result, the nonequilibrium magnons are created and with a bias increase up to $V = V_{c1}$ the magnetization is switched to the configuration $\mathbf{M}_a \uparrow \downarrow \mathbf{H}$. Such a configuration clearly is a nonequilibrium one and is supported only due to a presence of a current through the structure. This behavior can be accounted for within a framework of a classical spin-torque model. As for the magnon considerations, we have $eVS_z > 0$ since $S_z$ changes it sign with a reversal of $\mathbf{M}_a$. It means that formally the presence of the bias *increase* the magnon damping coefficient if the magnons are defined with respect to a new magnetization direction. The problem is that this new direction is not an equilibrium one. Thus, in a view that magnon excitations are defined with respect to equilibrium magnetization, the concept of magnons can hardly be applied to this antiparallel configuration. To describe the evolution of magnetization in this case one can use the Landau-Lifshitz-Gilbert approach (see, e.g., Ref. 5). In particular, it was shown that the following decrease of the bias magnitude leads to a switching to parallel configuration $\mathbf{M}_a \| \mathbf{H}$. So one sees a clear difference between $\mathbf{M} \| \mathbf{H} \rightarrow \mathbf{M} \uparrow \downarrow \mathbf{H}$ switching and $\mathbf{M} \uparrow \downarrow \mathbf{H} \rightarrow \mathbf{M} \| \mathbf{H}$ switching. While for the first process the magnon physics is relevant, it cannot be applied to the second process. As a result, there is an asymmetry of the hysteresis loop describing the switching. In particular, the branch involving nonequilibrium magnons is expected to contain gradual evolution while the other one does not. This is in excellent agreement with the experiments in Ref. 5.

We suggest the following experimental tests of our theory. In this we focus on the parallel magnetization configuration or configurations close to that, since for those the differences between our model and those based on the spin-torque approach are experimentally most accessible. Typically, the magnetizations of the spin-valve layers are aligned in a magnetic field applied parallel to the layers. To prevent strong modification of the magnon spectrum the field should just be high enough to arrange the alignment.

Formally, in the spin-torque model magnetization switching from a purely parallel configuration is impossible, so that already observation of switching would support the approach presented in this article. A complication seems to be that any fluctuation or pinning center may destroy the collinearity, so that the experiment would lose the capability to discriminate between the models. However, in the spin-torque models the

switching time depends on the angle $\beta$ characterizing the deviation from the collinear configuration as $\propto|\ln\beta|$. In contrast, this is not the case in our theory, which does not predict any significant dependence of the evolution on the initial angle between the magnetizations provided this angle is small and the value of $S_z$ corresponds to an almost collinear configuration. Thus, studies of the dependence of the switching time on $\beta$ (taking advantage of the angular tunability of the free layer) enable discrimination between our scenario and the spin-torque model.

Further, we propose a detailed analysis of the magnetization evolution in the initial stage of switching ($\theta \ll 1$ or $n_m \ll 1$). First, we note that according to the spin-torque model the evolution starts abruptly provided the current exceeds the critical value. In contrast, in our model, according to Eq. (4), a dramatic increase of $n_m$ is expected even at subcritical voltages $V<V_c$ provided the difference $|V-V_c|$ is small enough. To check this, we suggest to study the behavior of the magnetization with adiabatically slow increase of $V$.

Then, according to Eq. (29), in the spin-torque model the behavior of $\theta(t)$ or $\delta M(t)$ is purely exponential with $t$ until $\theta \sim 1$ or $\delta M \sim M$. In contrast, in our model after a period of exponential evolution [voltage controlled regime, Eq. (8)] the evolution is linear with $t$ [Eq. (8) corrected by Eq. (9)] and can include effects of magnon-magnon interactions discussed in Sec. III.

## VI. CONCLUSIONS

To conclude, we have given a consequent quantum-mechanical treatment of spin-polarized transport in a spin-valve point contact with an account of the induced nonequilibrium electron distribution. It is shown that at large biases an avalanchelike creation of low-frequency magnons within the ferromagnetic layer is possible which agrees with earlier predictions based on semiphenomenological models. However, in contrast to earlier studies,[1,2] it is found that the stabilization within the magnon system can be achieved at finite (although large) magnon occupation numbers and the gradual evolution of such a state with increasing bias is possible. We also explain a coexistence of the hysteretic and nonhysteretic behavior and a presence of telegraph noise even at low temperatures. Further, we predict an asymmetry of the hysteresis loop describing switching. These results are in agreement with existing experimental data. The comparison with existing theoretical models is given.

## ACKNOWLEDGMENTS

V.I.K. gratefully acknowledges the "Nederlandse Organisatie voor Wetenschappelijk Onderzoek (NWO)" for a visitors grant (Grant No. B67-332) and the Kavli Institute of Nanoscience Delft for hospitality. He also is grateful to U. S. Department of Energy Office of Science for financial support through Contract No. W-31-109-ENG-38 and to Argonne National Laboratory for hospitality.

## APPENDIX A: EFFECT OF FINITE THICKNESS AND DISORDER ON THE MAGNON-ELECTRON MATRIX ELEMENT

Following Mills *et al.*,[38] we write the matrix element for the transition of an electron in initial state $\mathbf{k}$ to final state $\mathbf{k}'$ due to creation of a magnon in state $\mathbf{q}$ as

$$g|_{\mathbf{k}\to\mathbf{k}'} = J\frac{\mathbf{s}\cdot\mathbf{M}}{sM}\frac{a^{3/2}}{\Omega^{3/2}}\int d\mathbf{r}\,\exp[i(\mathbf{k}-\mathbf{k}'-\mathbf{q})\cdot\mathbf{r}], \quad \text{(A1)}$$

where $\mathbf{s}$ ($s=\sigma\hbar$) and $\mathbf{M}$ are the electron spin and the magnetization, respectively, $J$ is the exchange constant, $a$ is the lattice constant, while $\Omega$ is the normalizing volume. Typically, the integration over the infinite sample volume in Eq. (A1) gives the standard momentum conservation law $\mathbf{k}=\mathbf{k}'+\mathbf{q}$. However, for the $x$ direction of the thin analyzer layer (see Fig. 1) the integration is over the finite range $t_a$. This leads to momentum nonconservation for this direction. The resulting matrix element renormalized with respect to momentum nonconservation due the finite thickness is denoted as $\tilde{g}$.

We assume that standard momentum conservation holds in plane of the layer, so that in Eq. (A1) we can concentrate on the integration over $x$. The corresponding factor arising in the expression for $|\tilde{g}|^2$ readily can be written as

$$\frac{a}{t_a^3(k_x-k_x'-q_x)^2}. \quad \text{(A2)}$$

For given initial and final electron energies $\varepsilon=\varepsilon_{\mathbf{k},-\sigma}$ and $\varepsilon'_{\mathbf{k}',\sigma}$ the Fermi surfaces are typically separated by a relatively large gap $|\mathbf{k}-\mathbf{k}'|=\Delta k_F \simeq k_F E_{\mathrm{ex}}/\varepsilon_F$. For magnons of long wavelength we expect $q \ll \Delta k_F$, which allows the neglect of $q$ in the estimates. We first integrate over $\vartheta,\vartheta'$ (denoting the angles of the wave vectors with respect to the $x$ axis) and $\varphi,\varphi'$ (denoting the angles of the wave vectors with respect to their in-plane component). Since the difference $\varepsilon-\varepsilon'$ (controlled by the distribution functions) is much less than $E_{\mathrm{ex}}$, we also will neglect this difference in course of the angular integrations. Thus one has $k_x=k_{F,-}\cos\vartheta$ and $k'_x=k_{F,+}\cos\vartheta'$. Momentum conservation in the analyzer plane of the layer eliminates integrations over $\varphi$ and $\varphi'$, with the obvious result $\sin\vartheta'=(k_{F,-}/k_{F,+})\sin\vartheta$ (which actually is the explicit expression for momentum conservation for the in-plane component). Correspondingly, one obtains

$$\cos\vartheta' = [1-(k_{F,-}/k_{F,+})^2\sin^2\vartheta]^{1/2}.$$

Since $k_{F,+}$ is larger than $k_{F,-}$, there clearly is a gap preventing small values of $\cos\vartheta'$. Further, one obtains for the denominator of Eq. (A2)

$$t_a^3k_F^2\left[\xi-\sqrt{\xi^2\left(1-2\frac{\Delta k_F}{k_F}\right)+2\frac{\Delta k_F}{k_F}}\right]^2 \simeq t_a^3k_F^2\left[\frac{\Delta k_F}{k_F}\left(\xi-\frac{1}{\xi^2}\right)\right]^2, \quad \text{(A3)}$$

where $\xi=\cos\vartheta$. Then, performing the integration over $\xi$, Eq. (A2) goes over into

$$\sim \frac{a}{t_a^3 \Delta k_F^2}.$$

Finally, after these manipulations $|\tilde{g}|^2$ can be obtained as

$$|\tilde{g}|^2 = J^2 \frac{k_F}{(\Delta k_F)^2 t_a}. \tag{A4}$$

The resulting rate equation taking into account this renormalization of the matrix element then is

$$\frac{dN_\omega}{dt} = \frac{1}{2\pi\hbar} \sum_\sigma \int d\varepsilon\, D(\varepsilon) \int d\varepsilon' D(\varepsilon') |\tilde{g}|^2 \times [f_{\varepsilon,\sigma}(1 - f_{\varepsilon',-\sigma})(1 + N_\omega)\delta(\varepsilon - \varepsilon' + \hbar\omega) - (1 - f_{\varepsilon,\sigma}) f_{\varepsilon',-\sigma} N_\omega \delta(\varepsilon - \varepsilon' - \hbar\omega_\alpha)], \tag{A5}$$

which is identical to Eq. (3). One notes that in view of the normalizing factors of the electron wave functions used in the course of matrix element calculation, one should also put $\Sigma_{\mathbf{k}} \propto t_a$, $\Sigma_{\mathbf{k}'} \propto t_a$, so that these factors eliminate the normalizing factor $t_a^2$ arising in the course of the estimate of $|\tilde{g}|^2$. This has been taken into account in Eq. (A5). The finite electron-magnon coupling strength for low magnon frequencies (and relatively small bias voltages) thus results from boundary-induced momentum nonconservation. Qualitatively, one may expect a similar effect from other factors breaking momentum conservation. The effect of alloy disorder significantly increases the efficiency of magnon-electron processes for low magnon frequencies.[38] Although in Ref. 38 disorder in the on-site exchange constant is considered, we show below that elastic electron scattering can enhance the coupling in a similar fashion.

We first consider the role of elastic scattering for a thin analyzer layer, $t_a < l_e$. Elastic scattering leads to modification of the electron wave functions with respect to the simple plane waves of the unperturbed problem due to emergence of a spherical scattered wave from each scattering site. In first order with respect to the scattering processes (which holds when $t_a < l_e$) the wave function is modified according to

$$e^{i\mathbf{k}\cdot\mathbf{r}} \to e^{i\mathbf{k}\cdot\mathbf{r}} + \sum_i f_i e^{i\mathbf{k}\cdot\mathbf{R_i}} \frac{e^{ik|\mathbf{r}-\mathbf{R_i}|}}{|\mathbf{r}-\mathbf{R_i}|}. \tag{A6}$$

Here $i$ numerates the scatterers, $\mathbf{R_i}$ is the coordinate of a scatterer, while $f$ is the scattering amplitude. Replacement of the plane waves in Eq. (A1) by the modified wave functions gives a nonzero result, even in the absence of the finite thickness effect. As before, we assume that $q \ll k, k'$, so that the integrand in the Eq. (A1) for each of the scatterer has the form

$$e^{i\mathbf{k}\cdot\mathbf{r}} e^{-i(\mathbf{k}'\cdot\mathbf{R_i} + k'|\mathbf{r}-\mathbf{R_i}|)} = e^{i(\mathbf{k}\cdot\mathbf{r}' + kr')} e^{i\Delta k r} e^{i(\mathbf{k}-\mathbf{k}')\cdot\mathbf{R_i}}, \tag{A7}$$

where $\mathbf{r}' = \mathbf{r} - \mathbf{R_i}$.

With the assumption $\Delta k \ll k$ the integration over $\mathbf{r}$ gives

$$\frac{A}{k\Delta k} \exp[i(\mathbf{k} - \mathbf{k}') \cdot \mathbf{R_i}], \tag{A8}$$

where $|A| \sim 1$. The total matrix element is obtained by summing over all scatterers in the layer. However, when squaring the element, products of contributions of different scatterers vanish due to the strongly oscillating factor in Eq. (A8) as a function of the scatterer coordinate. As a result, one finally obtains

$$|\tilde{g}|^2 \sim \frac{\varepsilon_F^2}{k_F l_e}. \tag{A9}$$

To obtain this estimate, we have used that $f^2 N_i \sim l_e^{-1}$ and that $J^2 \sim \varepsilon_F^2 (k_F/\Delta k)^2$. As it is seen, for $t_a < l_e$ the effect of scattering at elastic centers is smaller than the effect of boundary scattering. However, one expects that Eq. (A9) holds even for diffusive transport in the analyzer. Indeed, the contribution of each scatterer is actually formed at distances $\sim 1/(\Delta k)$ from the scatterer. So, the derivation implies ballistic transport only at the scale $1/(\Delta k)$, which is assumed to be less than $t_a$. In this case the electron-induced magnon relaxation rate with an account of the fact that $\Delta k \sim k_F (J/\varepsilon_F)$ can be estimated as

$$\tau_{m-e}^{-1} \simeq \frac{1}{k_F l_e} \omega. \tag{A10}$$

Thus we have in a natural way identified the factor $(1/k_F l_e)$ as the Gilbert damping parameter.

## APPENDIX B

Let us discuss a possible role of magnon-electron interactions. So far we assumed that the electron distribution given by Eq. (1) exists even at high magnon concentration. However, one can expect that a high magnon emission rate leads to decay in the analyzer of the spin-dependent part of the electron distribution. The latter consequently can no longer support further strong emission. To understand the evolution of this distribution with an increase of the magnon concentration we make use of the electron-magnon collision operator:

$$I_{e-m} = \int d\omega \int d\varepsilon' D(\varepsilon') \nu_\omega |\tilde{g}|^2 \{ f_{\varepsilon,\sigma}(1 - f_{\varepsilon',-\sigma})[(1 + N_\omega) \times \delta(\varepsilon - \varepsilon' - \hbar\omega) + N_\omega \delta(\varepsilon' - \varepsilon + \hbar\omega)] - f_{\varepsilon',-\sigma}(1 - f_{\varepsilon,\sigma}) \times [(1 + N_\omega)\delta(\varepsilon' - \varepsilon - \hbar\omega) + N_\omega \delta(\varepsilon - \varepsilon' + \hbar\omega)] \} \tag{B1}$$

Here $\nu(\omega)$ is the magnon density of states. As it is seen, for $N_\omega \gg 1$ with a neglect of the spontaneous processes this operator tends to establish an electron distribution of the sort $f_{\min}(\varepsilon) = f_{\mathrm{maj}}(\varepsilon - \hbar\omega)$. In addition, the electron-magnon processes even at very large $N_\omega$ can only take place between the electronic majority and minority states separated by the energy $\hbar\omega$ since the minority electron arising as a result of magnon absorbtion by the majority electron can not further absorb magnons and vice versa, the minority electron turning to the majority electron by an emission of magnon can not further emit magnons. Having these facts in mind one sees that, in particular, the integral of Eq. (B1) is cancelled by the electron distribution

$$f_{\mathrm{maj}} = \frac{1}{2}\left[ f_0\left(\varepsilon + \frac{eV}{2} + \hbar\omega\right) + f_0\left(\varepsilon - \frac{eV}{2}\right)\right],$$

$$f_{\mathrm{maj}} = \frac{1}{2}\left[ f_0\left(\varepsilon + \frac{eV}{2}\right) + f_0\left(\varepsilon - \frac{eV}{2} - \hbar\omega\right)\right]. \quad \text{(B2)}$$

So the electron-magnon coupling does not lead to a total decay of spin polarization, however the total density of polarized spins supported by the distribution resulting from the coupling in question is $\hbar\omega D$. Since the electrons effectively escape the analyzer layer, one expects that it is this spin density that describes the spin current leaving the layer. At the same time the incident spin current is controlled by initial electron distribution given by Eq. (1) which corresponds to the density of spins $\alpha eV/2D$. So one concludes that for $V > V_c$ the electron-magnon coupling within the analyzer however strong it is cannot suppress the spin pumping to the magnon system.

## APPENDIX C

In the point-contact geometry of Fig. 1 current passes only through a small region of the analyzer. While magnons are excited in the same region, they can escape it by propagating away into the analyzer plane. This differs from the situation in Refs. 1 and 2, where current flow and magnetization precession occur in the same volume. For point contacts, experimentally studied in Refs. 4, 6, and 39, an additional relaxation term $-N_\omega/\tau_m^{\mathrm{esc}}$ is added to Eq. (2), where $\tau_m^{\mathrm{esc}}$ is the magnon escape time given by $\tau_m^{\mathrm{esc}} = d/v_m = dm_m/\hbar q_m$. Here $v_m$ is the magnon velocity and $q_m$ is the magnon wave vector, which has the minimum value $\sim 1/d$. Correspondingly, the maximum value for $\tau_m^{\mathrm{esc}}$ is $d^2 m_m/\hbar$. The final effect of magnon escape is that $\tau_{m-e}/\tau_m^{\mathrm{esc}}$ appears as extra factor in the denominator of Eq. (4). This does not prevent divergence of $T_{m,\omega}^{\mathrm{eff}}$, but fast escape $(\tau_{m-e}/\tau_m^{\mathrm{esc}} \gg 1)$ leads to strong increase of the critical voltage according to

$$eV_c S_z = -(\tau_{m-e}/\tau_m^{\mathrm{esc}})\hbar\omega. \quad \text{(C1)}$$

Taking into account that $\tau_{m-e}^{-1} \simeq \omega/k_F t_a$ (see Appendix A) one obtains

$$\tau_{m-e}/\tau_{m-e}^{\mathrm{esc}} \geq \frac{k_F t_a}{\hbar\omega}\frac{\hbar^2}{d^2 m_m}, \quad \text{(C2)}$$

where the equality applies to the minimum magnon wave vector. Thus, in case of effective magnon escape $(\tau_{m-e}/\tau_{m-e}^{\mathrm{esc}} > 1)$, the critical voltage is independent of the magnon frequency. Further, the criticality starts at the lowest possible in-plane wave vector. Finally, we note that Eq. (C1) predicts $V_c \propto 1/d^2$. For a diffusive point contact (i.e., $R \propto 1/d^2$) the critical current is thus independent of the orifice size. This agrees with the prediction in Ref. 36, where the point-contact geometry is considered as well, but where spin transfer leads to coherent excitation of spin waves.


[1] J. C. Slonczewski, J. Magn. Magn. Mater. **159**, L1 (1996).
[2] L. Berger, Phys. Rev. B **54**, 9353 (1996).
[3] E. B. Myers, D. C. Ralph, J. A. Katine, R. N. Louie, and R. A. Buhrman, Science **285**, 867 (1999).
[4] S. J. H. C. Theeuwen, J. Caro, K. P. Wellock, S. Radelaar, C. H. Marrows, B. J. Hickey, and V. I. Kozub, Appl. Phys. Lett. **75**, 3677 (1999).
[5] J. A. Katine, F. J. Albert, R. A. Buhrman, E. B. Myers, and D. C. Ralph, Phys. Rev. Lett. **84**, 3149 (2000).
[6] M. Tsoi, A. G. M. Jansen, J. Bass, W.-C. Chiang, V. Tsoi, and P. Wyder, Nature (London) **406**, 46 (2000).
[7] S. I. Kiselev, J. C. Sankey, I. N. Krivorotov, N. C. Emley, R. J. Schoelkopf, R. A. Buhrman, and D. C. Ralph, Nature (London) **425**, 380 (2003).
[8] W. H. Rippard, M. R. Pufall, S. Kaka, T. J. Silva, S. E. Russek, and J. A. Katine, Phys. Rev. Lett. **95**, 067203 (2005).
[9] S. Urazhdin, N. O. Birge, W. P. Pratt, and J. Bass, Phys. Rev. Lett. **91**, 146803 (2003).
[10] S. Urazhdin, Phys. Rev. B **69**, 134430 (2004).
[11] S. Urazhdin, arXiv:cond-mat/0410520 (unpublished).
[12] A. Fabian, C. Terrier, S. S. Guisan, X. Hoffer, M. Dubey, L. Gravier, J. Ph. Ansermet, and J. E. Wegrowe, Phys. Rev. Lett. **91**, 257209 (2003).
[13] E. B. Myers, F. J. Albert, J. C. Sankey, E. Bonet, R. A. Buhrman, and D. C. Ralph, Phys. Rev. Lett. **89**, 196801 (2002).
[14] Z. Li and S. Zhang, Phys. Rev. B **69**, 134416 (2004).
[15] J. Xiao, A. Zangwill, and M. D. Stiles, Phys. Rev. B **72**, 014446 (2005).
[16] I. N. Krivorotov, N. C. Emley, J. C. Sankey, S. I. Kiselev, D. C. Ralph, and R. A. Buhrman, Science **307**, 228 (2005).
[17] X. Waintal, E. B. Myers, P. W. Brouwer, and D. C. Ralph, Phys. Rev. B **62**, 12317 (2000).
[18] S. Zhang, P. M. Levy, and A. Fert, Phys. Rev. Lett. **88**, 236601 (2002).
[19] M. D. Stiles and A. Zangwill, Phys. Rev. B **66**, 014407 (2002).
[20] J. C. Slonczewski, J. Magn. Magn. Mater. **247**, 324 (2002).
[21] J. Barnas, A. Fert, M. Gmitra, I. Weymann, and V. K. Dugaev, Phys. Rev. B **72**, 024426 (2005).
[22] Y. Tserkovnyak, A. Brataas, and G. E. W. Bauer, Phys. Rev. Lett. **88**, 117601 (2002).
[23] Y. Tserkovnyak, A. Brataas, and G. E. W. Bauer, Phys. Rev. B **66**, 224403 (2002).
[24] Y. Tserkovnyak, A. Brataas, and G. E. W. Bauer, Phys. Rev. B **67**, 140404(R) (2003).
[25] Ya. B. Bazaliy, B. A. Jones, and S. C. Zhang, J. Appl. Phys. **89**, 6793 (2001).
[26] J. Z. Sun, Phys. Rev. B **62**, 570 (2000).
[27] I. O. Kulik and R. I. Shekhter, Sov. J. Low Temp. Phys. **6**, 88 (1980).
[28] A. I. Akimenko and I. K. Yanson, Pis'ma Zh. Eksp. Teor. Fiz. **31**, 209 (1980) [JETP Lett. **31**, 198 (1980)].
[29] I. O. Kulik and I. K Yanson, Sov. J. Low Temp. Phys. **4**, 596 (1978).
[30] A. I. Akhiezer, V. G. Baryakhtar, and S. V. Peletminskii, *Spin Waves*, North-Holland Series in Low Temperature Physics Vol. 1 (North-Holland, Amsterdam, 1968).
[31] Daniel Huertas Hernando, Yu. V. Nazarov, Arne Brataas, and Gerrit E. W. Bauer, Phys. Rev. B **62**, 5700 (2000).

[32] A. A. Kovalev, G. E. W. Bauer, and A. Brataas, Phys. Rev. B **75**, 014430 (2007).
[33] M. D. Stiles, Jiang Xiao, and A. Zangwill, Phys. Rev. B **69**, 054408 (2004).
[34] M. L. Polianski and P. W. Brouwer, Phys. Rev. Lett. **92**, 026602 (2004).
[35] S. V. Gantsevich, V. L. Gurevich, V. D. Kagan, and R. Katilius, Phys. Status Solidi B **75**, 407 (1976).
[36] J. C. Slonczewski, J. Magn. Magn. Mater. **195**, L261 (1999).
[37] Sh. Kogan, Phys. Rev. Lett. **81**, 2986 (1998).
[38] D. L. Mills, A. Fert, and I. A. Campbell, Phys. Rev. B **4**, 196 (1971).
[39] M. Tsoi, A. G. M. Jansen, J. Bass, W. C. Chiang, M. Seck, V. Tsoi, and P. Wyder, Phys. Rev. Lett. **80**, 4281 (1998).